Tight-binding electronic-structure calculations and tight-binding molecular dynamics with localized orbitals

S. Goedecker
Cornell Theory Center, Ithaca, New York 14853-3801

M. Teter
Laboratory of Atomic and Solid State Physics, Cornell University, Ithaca, New York 14853-3801
and Corning Inc., Corning, New York 14831

(Received 12 August 1994)

We describe in detail and extend our recent algorithm for tight-binding total-energy calculations and tight-binding molecular dynamics, which scales quadratically with the size of the system for small systems and linearly for big systems. It is intrinsically parallel and gives an excellent performance on parallel computers. The central quantity in this algorithm is the localized orbitals. We show in the context of various examples, that our localized-orbital algorithm is not only fast, but gives us also a better physical understanding than conventional extended orbitals and more flexibility in treating complicated geometries. The algorithm can also efficiently handle metallic systems and does not lead to unphysical distortions of the electronic density of states around the Fermi level.

I. INTRODUCTION

The tight-binding (TB) method[1] is a widely used electronic-structure method and has proven its usefulness for a wide range of systems ranging from transition metals to covalent materials. When a suitable repulsive potential is added, the TB method can also be used for tight-binding molecular-dynamics (TBMD) simulations.[2] The main advantage of the TB method is that it is significantly faster than *ab initio* density-functional calculations[3] and Car-Parrinello molecular-dynamics simulations[4] but still gives accurate enough results in many cases. There are, however, situations where one needs a huge number of time steps in a molecular-dynamics simulation, or where one wants to treat very big systems. In these cases, computer time, even with the TB method, can become a problem if one uses traditional algorithms such as standard diagonalization techniques or Car-Parrinello-type fictitious Lagrangian dynamics. The first case poses a problem because traditional algorithms are usually implemented only for serial machines. It is, therefore, not possible to take advantage of powerful parallel machines to speed up a single time step in the molecular-dynamics simulation. The fact that there are few parallel implementations is related to the difficulty in parallelizing traditional algorithms. The second case is difficult to handle with standard techniques because they have a scaling of the computational effort, which is cubic with respect to the number of atoms; therefore, the computer time grows much faster than the size of the system. This problem of the cubic scaling has been recognized by the computational-physics community and several proposals have recently been put forward to overcome this bottleneck.[5]

In this paper, we will describe in detail a recent algorithm[6] and extend it to metallic systems. The algorithm is extremely easy to implement on parallel computers and gives a speedup that is nearly proportional to the number of processors. Therefore, it can significantly reduce the computational time required for one time step in TBMD simulation for systems of any size. In addition, for large systems it scales linearly with the number of atoms for both insulators and metals. For large systems, it is faster than the traditional techniques even on a serial computer. Our approach is based on a projection rather than on minimization. It allows us to attack complicated problems in physically very intuitive way. It is also free of numerically cumbersome local minima, which are found in restricted minimization schemes.

Since the tight-binding method is not highly accurate, it is not necessary to calculate quantities with very high precision. In this paper, we adjust all numerical parameters such that we obtain a precision of 10 meV in the total energy per atom. In this way, the error from the algorithm is certainly always smaller than the error from the tight-binding method itself. As is well known, energy differences are always much more precise than the total energy itself.

II. THE ALGORITHM TO CALCULATE THE FERMI MATRIX

The central object in this algorithm is the finite-temperature density or Fermi matrix. All other quantities such as energies, charges, and forces can be formulated in terms of the Fermi matrix and its calculation takes most of the CPU time. The Fermi matrix $F_{\mu,T}$ is given by

$$F_{\mu,T}=f\left[\frac{H-\mu}{kT}\right],$$

where $f[(\epsilon_i-\mu)/(kT)]$ is the Fermi-Dirac distribution. The Hamiltonian matrix H is of dimension $m\times m$ and

each of its columns and rows is labeled by the double index $l\alpha$, where α denotes a particular atom and l denotes the quantum numbers of the Löwdin orbital $\varphi_{l\alpha}$ centered on the αth atom.

The Fermi matrix is diagonal in the eigenfunction representation

$$\langle \Psi_i | F_{\mu,T} | \Psi_j \rangle = f\left[\frac{\epsilon_i - \mu}{kT}\right]\delta_{i,j} , \quad (1)$$

where ϵ_i are the eigenvalues and Ψ_i the eigenvectors obtained from the TB Hamiltonian H ($H\Psi_i = \epsilon_i \Psi_i$). In this algorithm, the Fermi matrix is expressed as a matrix polynomial in H:

$$F_{\mu,T} = p_{\mu,T}(H) . \quad (2)$$

Clearly $p_{\mu,T}(H)$ is also diagonal in the usual eigenfunction representation:

$$\langle \Psi_i | p_{\mu,T}(H) | \Psi_j \rangle = p_{\mu,T}(\epsilon_i)\delta_{i,j} . \quad (3)$$

Comparing Eqs. (1) and (3), we see that the polynomial $p_{\mu,T}(\epsilon)$ has to approximate the Fermi distribution in the energy interval where the Hamiltonian has its eigenvalues. In our implementation $p_{\mu,T}(\epsilon)$ is a Chebyshev polynomial, which approximates the electronic weight distribution. If finite-electronic-temperature effects are to be taken into the account, the electronic weight distribution is of course the Fermi distribution. In most cases, however, one deals with nearly zero electronic temperature. Representing a step function by a finite-degree polynomial is not possible. Fortunately, this is not necessary. In the case of an insulator, the only requirement is that the electronic weight distribution be one in the valence-band region and zero in the conduction-band region. In the band gap it can vary smoothly from one to zero. In this situation, we represent the electronic weight distribution by a Chebyshev polynomial, which approximates the complementary error function $\frac{1}{2}\mathrm{erfc}[(\epsilon-\mu)/\Delta\epsilon]$, where typically $\Delta\epsilon \approx g/2$, where g is the band gap. Since we are not interested in the effects of a finite electronic temperature, we chose the complementary error function rather than the finite-temperature Fermi distribution because the former approaches one and zero faster in the band regions and is nevertheless easy to expand in a Chebyshev polynomial. The degree of the polynomial n_{pl} is then chosen to be

$$n_{\mathrm{pl}} = C\frac{\epsilon_{\max} - \epsilon_{\min}}{\Delta\epsilon} ,$$

where $C \approx 2$. The resulting electronic weight distribution is shown in Fig. 1 for the case of diamond.

The convergence of the band-structure energy with respect to $\Delta\epsilon$ has an exponential behavior and low-order polynomials ($n_{\mathrm{pl}} \approx 50$) are, therefore, accurate enough to obtain our target precision of 10 meV, as shown in Fig. 2.

In the case of a metal we can use the same weight distribution. From the Sommerfeld expansion, we know that the error introduced by a finite temperature is proportional to $(kT)^2$ and we expect that in this case the error will be proportional to $(\Delta\epsilon)$ as well,[2] which is

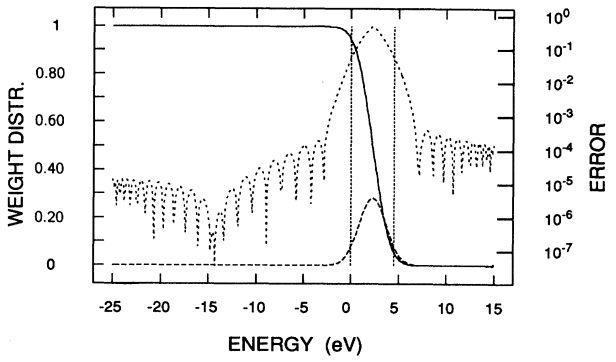

FIG. 1. The electronic weight distribution (solid line) as given by a Chebyshev polynomial of 40°. It was obtained by a fit to the function erfc. The dashed line is the negative derivative of the polynomial and the dotted line is the error with respect to a step function (zero-temperature Fermi distribution). The gap is shown by the horizontal lines. The error is large in the band gap, medium in the band-edge region where the density of states is still small, and very small in the band region.

confirmed by the numerical tests shown in Fig. 3. The degree n_{pl} necessary to obtain the target accuracy is typically of the order of 150 in a metal. Metals with a very complicated Fermi surface would probably require even higher-degree polynomials since their density of states varies rapidly around the Fermi level. In a metal, one has also to determine the exact position of the Fermi level, which gives charge neutrality. This requires some additional iterations with different polynomials corresponding to different Fermi levels.

Let us now discuss how to calculate the matrix polyno-

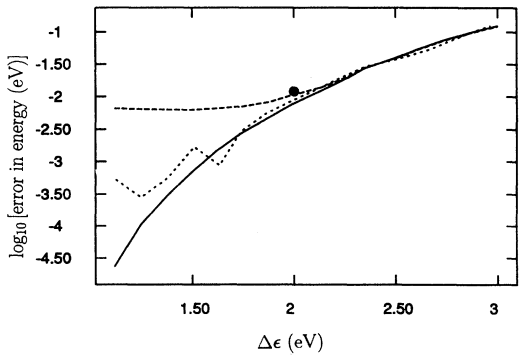

FIG. 2. The convergence of the band-structure energy as a function of the steepness $\Delta\epsilon$ of the electronic weight distribution for diamond. The gap from the tight-binding parametrization is 4 eV. The full line is the result for an infinite localization region and a highly accurate polynomial ($C=3$); the dashed line is the result if a localization region of radius 6.5 Å is used with the same polynomial; the dotted line is again for an infinite localization region, but for a moderately accurate polynomial with $C=2$. The recommended choice of the parameters $\Delta\epsilon = g/2$, $C=2$, and $r_{\mathrm{loc}}=6.5$ gives, therefore, an accuracy of 10 meV as indicated by the point. Since $\epsilon_{\max} - \epsilon_{\min}$ is roughly 40 eV, $n_{\mathrm{pl}}=40$.

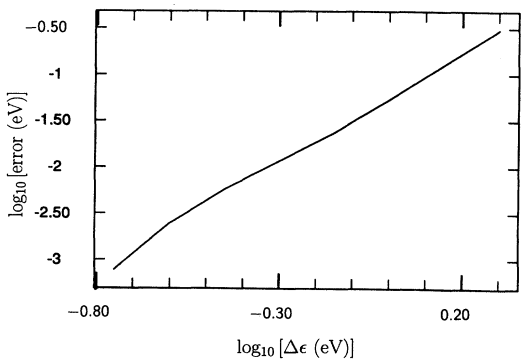

FIG. 3. The convergence of the band-structure energy for a crystalline system of 4000 Al atoms on a double logarithmic scale (base 10). Harrison's (Ref. 7) universal tight-binding parameters were used. The numerically observed convergence is actually slightly faster than the expected quadratic convergence. A polynomial of 110° is necessary to obtain the target accuracy of 10 meV per atom.

mial $p_{\mu,T}(H)$, which is expanded in Chebyshev polynomials T_j,

$$p_{\mu,T}(H)=\frac{c_0}{2}+\sum_{j=1}^{n_{\rm pl}} c_j T_j(H) \ . \tag{4}$$

The Chebyshev matrix polynomials satisfy the recursion relations

$$T_0(H)=I \ ,$$
$$T_1(H)=H \ ,$$
$$T_{j+1}(H)=2HT_j(H)-T_{j-1}(H) \ ,$$

where I is the identity matrix. The $l\alpha$th column of the matrix $T_j(H)$ denoted by $|t_{l\alpha}^j\rangle$ can, therefore, be calculated by the same recursion

$$|t_{l\alpha}^0\rangle=|\varphi_{l\alpha}\rangle \ ,$$
$$|t_{l\alpha}^1\rangle=H|\varphi_{l\alpha}\rangle \ , \tag{5}$$
$$|t_{l\alpha}^{j+1}\rangle=2H|t_{l\alpha}^j\rangle-|t_{l\alpha}^{j-1}\rangle \ ,$$

where $|\varphi_{l\alpha}\rangle$ denotes a unit vector whose only nonzero element is the element corresponding to the Löwdin orbital $l\alpha$. Once the vectors $|t_{l\alpha}^j\rangle$ are calculated, one just has to form the linear combinations according to Eq. (4) to obtain the corresponding column of the Fermi matrix. Denoting this column by $|f_{l\alpha}\rangle$, this can be written as

$$|f_{l\alpha}\rangle=F|\varphi_{l\alpha}\rangle\approx p_{\mu,T}(H)|\varphi_{l\alpha}\rangle$$
$$=\frac{c_0}{2}|t_{l\alpha}^0\rangle+\sum_{j=1}^{n_{\rm pl}} c_j|t_{l\alpha}^j\rangle \ . \tag{6}$$

To calculate one column of the Fermi one has essentially to do a sequence of $n_{\rm pl}$ matrix times vector multiplication [Eq. (5)]. In the tight-binding context, the Hamiltonian matrix is a sparse matrix whose number of off-diagonal elements $n_{\rm off}$ is equal to the number of interacting orbitals on the neighboring atoms. In the case of diamond, there are four nearest neighbors with four orbitals each; thus, the Hamiltonian has 16 off-diagonal elements.

It is immediately seen that the calculation of one sequence of columns $|t_{l\alpha}^j(H)\rangle$, $j=0,\ldots,n_{\rm pl}$ is completely independent from the calculation of another sequence $|t_{l',\alpha'}^j(H)\rangle$, $j=0,\ldots,n_{\rm pl}$. This is the reason why the algorithm is intrinsically parallel and, therefore, well suited for parallel computers.

As has been described, the algorithm scales quadratically with the number of atoms in the system. If there are m orbitals in the system, the effort required to calculate the full $m\times m$ density matrix is evidently proportional to $m^2 n_{\rm pl} n_{\rm off}$.

By taking advantage of the decay properties of the Fermi matrix, one can, however, obtain a linearly scaling scheme. As has been known for a long time, Wannier functions decay exponentially in insulators,[8] the decay constant being proportional to $\sqrt{g}$. The Wannier functions are just an alternative set of functions spanning the space of all the occupied one-particle electron wave functions. Now at zero temperature, the Fermi matrix is a projection operator cutting out all the components belonging to eigenfunctions above the Fermi level and leaving only the components below the Fermi level. As argued by Vanderbilt,[9] the vector $F|\varphi_{l\alpha}\rangle$, which is one column of the Fermi matrix, has to be a linear combination of the Wannier functions and should decay exponentially. Numerical testing shows indeed that for an insulator the off-diagonal elements decay exponentially (Fig. 4).

Because of these relations we will, from now on, call a column of the Fermi matrix $|f_{l\alpha}\rangle$ a localized orbital. This rapid decay of the localized orbitals allows us to introduce a certain cutoff radius $r_{\rm loc}$ outside of which the amplitude of the localized orbital is negligible. The volume, where the localized orbital is not negligible, will be called the localization region. Coming back to the Fermi matrix, this means that we can consider the Fermi matrix to be a sparse matrix with $m_{\rm loc}$ off-diagonal elements, where $m_{\rm loc}$ is the number of orbitals in the localization region. The numerical effort to calculate the Fermi matrix is, therefore, proportional to $m m_{\rm loc} n_{\rm pl} n_{\rm off}$. In-

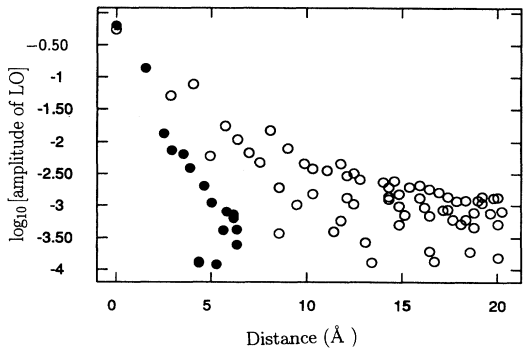

FIG. 4. Decay of the LO's in C (full discs) and Al (open discs).

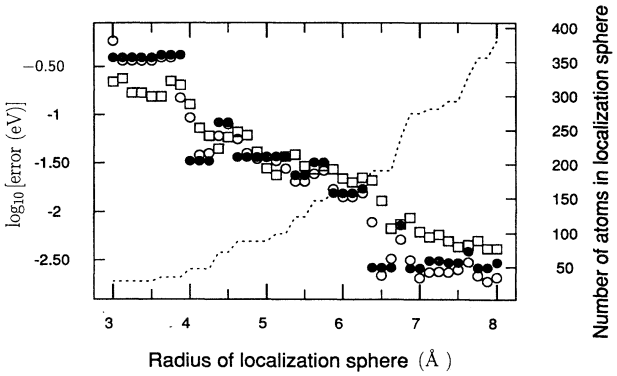

FIG. 5. Convergence of relevant quantities on a logarithmic scale (base 10) as a function of the radius of the localization sphere for a carbon system. The full discs show the convergence of the absolute total energy in eV for a perfectly ordered diamond structure; the open discs show the same quantity for a slightly randomly disordered crystal; the squares show the relative error of the forces for the same disordered crystal; the dotted line shows the number of atoms in the localization region as a function of its radius.

stead of carrying out the recursions of Eq. (5) over the whole volume of the system, they are done in the localization region only. Reflecting boundary conditions are used at the surface of the localization sphere. If the volume of the system is larger than the localization volume, only m increases with the number of atoms in the system; the method is, therefore, linear. The convergence of the total energy and the forces as a function of the size of the localization region in an insulator is shown in Fig. 5. To obtain total energies with an error of 10 meV and two correct digits in the forces, a localization radius of 6.5 Å is required.

In a metal the localized orbitals decay algebraically. This slow decay can be traced back to the discontinuity of the Fermi distribution at zero temperature. As we have seen, we can replace the sharp Fermi distribution by a smooth version without introducing large errors. The localized orbitals calculated from such a smoothed out electronic weight distribution show again an exponential decay proportional to $\sqrt{\Delta\epsilon}$ (Fig. 4). This artificial decay is usually much slower than in the case of an insulator, since $\Delta\epsilon$ is rather small. Unless one goes to very large systems, the localization region will never be smaller than the volume of the system and one will observe a quadratic scaling rather than a linear one.

III. BAND-STRUCTURE ENERGY, OCCUPANCY, AND FORCES

Let us now derive the physically interesting quantities. Within the TBMD scheme, the total energy $E_{\rm tot}$ of a given system is expressed as

$$E_{\rm tot}=\sum_{\alpha}\frac{p_\alpha^2}{2m_\alpha}+\sum_i \epsilon_i f\left[\frac{\epsilon_i-\mu}{kT}\right]+U_{\rm rep}\ , \tag{7}$$

where the first term is the kinetic energy of the ions and $U_{\rm rep}$ is a suitable repulsive potential. The contribution from the classical potential $U_{\rm rep}$ is easy to calculate and we will, therefore, concentrate on the sum over the eigenvalues, which is also called the band-structure energy.

The band-structure energy can be expressed as

$$E_{\rm bs}={\rm Tr}[HF]=\sum_{l\alpha}\langle\varphi_{l\alpha}|HF|\varphi_{l\alpha}\rangle=\sum_{l\alpha}\langle H\varphi_{l\alpha}|f_{l\alpha}\rangle\ . \tag{8}$$

The equivalence of the two expressions for the band-structure energy in Eqs. (7) and (8) follows readily from the fact that the trace is invariant under the unitary transformation from the Ψ_i representation to the $\varphi_{l\alpha}$ representation, and that the Fermi matrix is diagonal in the basis set of the eigenfunctions Ψ_i. With this form, the energy can be decomposed in a physically intuitive way into the contributions from each atom α given by $\sum_l\langle H\varphi_{l\alpha}|f_{l\alpha}\rangle$. The energy of each atom depends only on the localized orbitals centered on this atom.

In an analogy to the band-structure energy, the total number of electrons is given by

$$N={\rm Tr}[F]=\sum_{l\alpha}\langle\varphi_{l\alpha}|F|\varphi_{l\alpha}\rangle=\sum_{l\alpha}\langle\varphi_{l\alpha}|f_{l\alpha}\rangle\ . \tag{9}$$

One diagonal element of the Fermi matrix $\langle\varphi_{l\alpha}|F|\varphi_{l\alpha}\rangle$ gives the occupancy of the orbital $\varphi_{l\alpha}$. The sum $\sum_l\langle\varphi_{l\alpha}|f_{l\alpha}\rangle$ gives the charge associated with atom α. Again it is only the set of orbitals centered on atom α that determines its charge. It is useful that the local charge can easily be calculated since some versions of the tight-binding method require local-charge neutrality.

The force acting on an atom is again a sum of a contribution arising from a classical repulsive energy, which is trivial, and the band-structure energy. The second contribution is also called the Hellman-Feynman force $\mathbf{f}_\beta$; it is the derivative of $E_{\rm bs}$ with respect to the atomic displacements $\mathbf{R}_\beta$

$$\begin{aligned}\mathbf{f}_\beta&={\rm Tr}\left[[p_{\mu,T}(H)+Hp'_{\mu,T}(H)]\frac{\partial H}{\partial\mathbf{R}_\beta}\right]\\&=\sum_{l\alpha}\sum_{l'\alpha'}\langle\varphi_{l\alpha}|[p_{\mu,T}(H)+Hp'_{\mu,T}(H)]|\varphi_{l'\alpha'}\rangle\\&\quad\times\langle\varphi_{l'\alpha'}|\frac{\partial H}{\partial\mathbf{R}_\beta}|\varphi_{l\alpha}\rangle\ ,\end{aligned}$$

where $p'_{\mu,T}$ is the derivative of $p_{\mu,T}$. The matrix $p'_{\mu,T}(H)$ can be calculated analogously to the matrix $p_{\mu,T}(H)$. In the nearest-neighbor tight-binding method, the hopping matrix elements between neighboring atoms are scaled with the interatomic distance according to the Harrison rule. The matrix elements $\langle\varphi_{l'\alpha'}|\partial H/\partial\mathbf{R}_\beta|\varphi_{l\alpha}\rangle$, therefore, vanish unless either α equals β and α' is a nearest neighbor of β, or α' equals β and α is a nearest neighbor of β. Introducing an index γ, which runs over all the nearest neighbors of β, and using the symmetry of the matrices, we obtain

$$\mathbf{f}_\beta = 2\sum_\gamma \sum_{l,l'} \langle \varphi_{l'\gamma} | [p_{\mu,T}(H) + Hp'_{\mu,T}(H)] | \varphi_{l\beta} \rangle \times \langle \varphi_{l'\gamma} | \frac{\partial H}{\partial \mathbf{R}_\beta} | \varphi_{l\beta} \rangle \tag{10}$$

$$= 2\sum_\gamma \sum_{l,l'} \langle \varphi_{l'\gamma} | g_{l\beta} \rangle \langle \varphi_{l'\gamma} | \frac{\partial H}{\partial \mathbf{R}_\beta} | \varphi_{l\beta} \rangle ,$$

where $|g_{l\beta}\rangle = [p_{\mu,T}(H) + Hp'_{\mu,T}(H)]|\varphi_{l\beta}\rangle$ is another kind of localized orbital, which is, however, identical to $|f_{l\beta}\rangle$ in the case of an insulator at zero temperature. This means that the force acting on atom β depends only on the amplitudes of the localized orbitals $|g_{l\beta}\rangle$ centered on atom β. Since all the dependence of the band-structure energy upon the atomic positions enters through the scaling of the Hamiltonian matrix elements, there are no Pulay forces in this scheme.

As we saw, the algorithm allows us to calculate the force as the exact derivative of the approximate energy. This guarantees that the forces vanish at the equilibrium configuration. It also leads to a highly accurate conservation of the total energy in a MD simulation (Fig. 6). Statistical quantities that depend on the fluctuations of the energy such as the specific heat can, therefore, be calculated. The small deviations from exact energy conservation arise mainly when atoms enter or leave the localization volume of radius 6.5 Å between two time steps. In the case of a metal, the total energy is only conserved if the simulation is done at constant chemical potential. For a sufficiently large system, the chemical potential should of course not vary unless other thermodynamic variables such as temperature or pressure are changed and a constant chemical potential implies a constant number of electrons. In a finite system, however, the number of electrons fluctuate around the average neutrality level (Fig. 6). In an insulator at sufficiently temperature, both total energy and the number of electrons are conserved to very high precision.

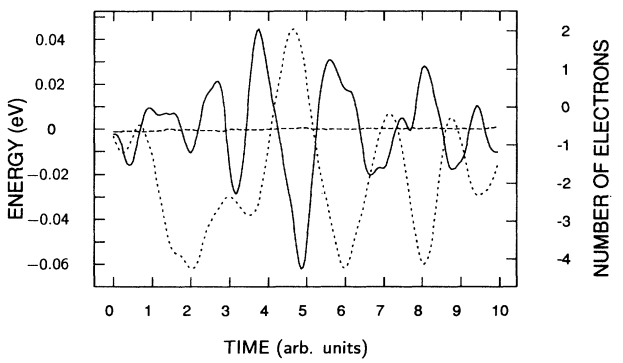

FIG. 6. Conservation of the total energy in a molecular-dynamics simulation of a liquid-carbon sample containing 512 atoms at a temperature of 5000 K and for fixed chemical potential. The deviations from exact energy conservation (dashed line) are more than two orders of magnitude smaller than the oscillations of the kinetic energy of the ions around its average value (solid line). The dotted line gives the fluctuations of the number of electrons around the charge-neutrality value.

IV. DENSITY OF STATES AND ITS MOMENTS

The density of states can be reconstructed from its moments M_ν, where

$$M_\nu = \sum_i \epsilon_i^\nu . \tag{11}$$

For reasons of numerical stability, it is preferable not to use the moments themselves but, instead, moments with respect to well-behaved polynomials such as the Legendre polynomials L_ν. We will assume in the following that the Hamiltonian matrix was scaled in such a way that all eigenvalues are in the interval $[-1;1]$. The numerically stable moments are then

$$M_\nu = \sum_i L_\nu(\epsilon_i) . \tag{12}$$

Let us now expand the density of states $D(\epsilon)$ in Legendre polynomials:

$$D(\epsilon) = \sum_\nu d_\nu L_\nu(\epsilon) . \tag{13}$$

The expansion coefficients d_ν are then given by

$$d_\nu = \frac{2\nu+1}{2} \int_{-1}^{1} D(\epsilon) L_\nu(\epsilon) d\epsilon . \tag{14}$$

Using the properties of the trace and the definition of the density of states, we obtain

$$\mathrm{Tr}[L_\nu(H)] = \sum_i L_\nu(\epsilon_i) \approx \int_{-1}^{1} D(\epsilon) L_\nu(\epsilon) d\epsilon . \tag{15}$$

This means that the moments M_ν are the expansion coefficients of the density of states and they can be calculated by taking the trace of the Legendre polynomial of the Hamiltonian matrix. The approximate equal sign in Eq. (15) comes from the fact that the sum can be replaced by the integral only in the limit of an infinitely large system. Since we are, however, interested in very large systems, the approximation is very good.

The trace over matrices $L_\nu(H)$ with high values of ν gives the short-wavelength details of the band structure. These matrices are much less diagonally dominant than the Fermi matrix; unless one considers huge systems, it is not possible to cut them off at a radius smaller than the radius of the system. This is not surprising. In a periodic crystal, the Fourier coefficients $E(\mathbf{R})$ of the band-structure $E(\mathbf{k})$ are given by

$$E(\mathbf{R}) = \int W(\mathbf{r}) W H(\mathbf{r} - \mathbf{R}) d\mathbf{r} ,$$

where $\mathbf{R}$ is a lattice vector and W a Wannier function. High Fourier coefficients and, therefore, short-wavelength details of the band structure are determined by the long-range tail of the Wannier function. Zeroing the Wannier functions outside a certain radius corresponds to zeroing high Fourier coefficients of the band structure. Details of the density of states are, thereby, of course also lost.

Crystalline systems have van Hove singularities in the density of states. These singularities are difficult to ap-

proximate by a polynomial such as in Eq. (13). In this case, other methods such as the recursion[10] method, which also reconstruct the density of states from its moments, give certainly better results. For large noncrystalline systems the method works, however, very well. For a smooth density of states, the exact coefficients d_ν decay for increasing ν. The numerical coefficients start, however, increasing again from a certain point because the approximate equality in Eq. (15) does not hold any more. This point is the optimal point to truncate the numerical expansion in Eq. (13). The density of states during one time step of a MD simulation of liquid carbon is shown in Fig. 7.

The method allows us again to zoom into the local density of states of each atom α, whose moments are given by

$$\sum_l \langle \varphi_{l\alpha} | L_\nu(H) | \varphi_{l\alpha} \rangle \ .$$

Recently another method[13] was proposed where the density of states was constructed through its polynomial moments. In this work, Chebychev polynomials were used instead of the Legendre polynomials used here. For Chebychev polynomials, Eq. (15) does not hold and one has to resort to more complicated integration schemes to determine the expansion coefficients of the density of states. In principle, one can also calculate the band-structure energy by integration over the density of states as it is given by the polynomial expansion. This approach[13] is, however, much less accurate and gives very unreliable forces. The reason for this is that the change of a single level leads to a slight modification of the whole density of states, which leads to spurious forces. The preferred method for forces (as described in the previous sections) is, therefore, to do a polynomial expression of the Fermi matrix instead of the density of states. Since the polynomial expansion of the Fermi matrix does not depend on the atomic positions, there are no spurious contributions to the forces.

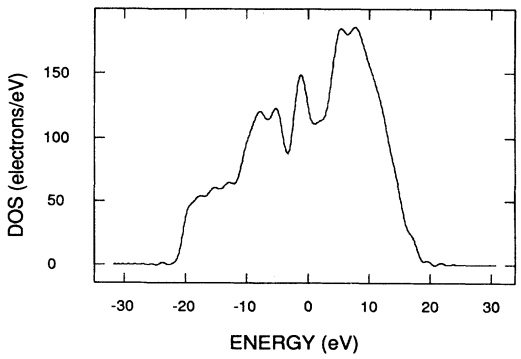

FIG. 7. The electronic density of states of a sample of 1000 carbon atoms in the liquid low-density phase at 5000 K. Legendre polynomials up to degree 77 were used.

V. PERFORMANCE EVALUATION

Whereas the CPU time required to do a TB calculation with standard diagonalization depends only on the number of atoms in the systems, it depends both on the number and type of atoms if our algorithm is used. Metals are slower than insulators because they are usually found in closed-packed structures with many nearest neighbors, the localization volume is much larger, and a higher-order degree polynomial is required. The timing results for our target precision are shown in Fig. 8.

It is seen that the algorithm is faster for any reasonable number of carbon atoms. The timing curve shows first a quadratic behavior, which goes over into a linear one as the size of the system becomes larger than the localization volume. A localization radius of 6.5 Å and a polynomial of degree 40 was used. In the case of the metal, the transition from quadratic to linear behavior occurs much later because of the larger localization volume of 12 Å. Because of the higher-degree polynomial ($n_{\rm pl}=110$) and the 12 nearest neighbors, the algorithm is, however, slower than traditional diagonalization for systems containing less than 180 atoms. By requiring a lower precision and especially a smaller localization volume, the timings can, of course, be significantly reduced in both cases. Because of the intrinsic parallelism of the algorithm, nearly linear speedup can be obtained with the method on parallel computers.[11]

VI. LOCALIZED ORBITALS FOR VARIOUS PROBLEMS

A. Crystalline materials

Standard methods are completely adequate for crystals with small elementary cells and the following discussion is, therefore, mainly intended to foster a better understanding of the localized-orbital (LO) method. Let us consider a simple crystal with one atom per elementary cell. To calculate the electronic structure of the bulk ma-

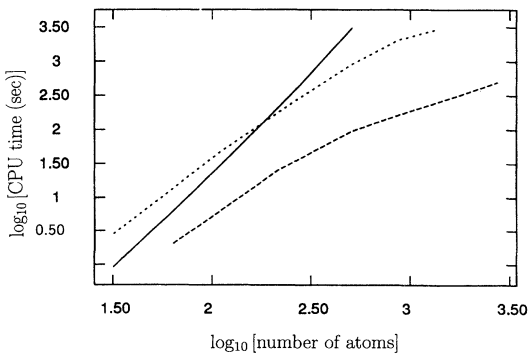

FIG. 8. The measured execution times for systems containing between 32 and 2744 atoms on a double logarithmic scale ($\log_{10}$). The solid line shows the execution time for standard diagonalization. The timings obtained with our algorithm are shown by the dotted line for a system of Al atoms and by the dashed line for a system of C atoms.

terial with standard methods, one considers a large enough periodic volume containing several elementary cells. Because of Bloch's theorem, solving the Schrödinger equation for this periodic volume is equivalent to solving Schrödinger's equation in the small elementary cell for several k points in the Brillouin zone. Since one k-point calculation is independent from the other, the numerical effort grows linearly with the number of elementary cells in the periodic volume and one can, therefore, easily approach the bulk behavior corresponding to an infinite periodic volume. Let us now discuss how to do the same calculation with localized orbitals. Because of symmetry, all LO's with the same quantum number l, but centered on different atoms are equal. It is, therefore, only necessary to calculate one set of LO's centered on a particular atom. The other atoms just have to backscatter the tails of this set of LO's. As one increases the localization volume of this set of LO's, one approaches the bulk behavior. Increasing the localization volume corresponds, therefore, to adding more k points in the classical approach. With our approach, the numerical effort increases linearly with the localization volume and one can, therefore, again easily obtain the limiting bulk behavior. This leads us to an important conclusion. The localization volume is the volume where a system starts to show bulklike behavior. The last statement remains true in noncrystalline systems such as amorphous systems. For pure electronic-structure calculations, it does not make sense to calculate systems larger than the localization volume and one will not be able to take advantage of the linear scaling. Because our algorithm shows quadratic behavior for systems smaller than the localization volume and because it is parallelizable, it is already advantageous to use it for smaller systems.

B. Annihilation of two screw dislocations in silicon

Localized-orbital methods can demonstrate their superiority for large and complicated systems without an easy crystalline structure. A system we consider in this class of problems are two screw dislocations in silicon. Arias and Joannopoulos[12] recently reported *ab initio* density-functional calculations for this system in a supercell containing 324 atoms. This system size is currently near the limit of what can be done with state of the art *ab initio* techniques, whereas it is only a moderate-size calculation with the our TB method. As shown in Table I the tight-binding scheme[2] gives very similar results for the energy of the dislocations at different separations. Since the computational workload is much smaller, larger cells can be used to test the convergence with respect to the number of k points. The TB model also predicts, in agreement with *ab initio* results, that a pair of screw antiscrew dislocations along the 110 axis will annihilate if their separation is 3.3 Å.

Arias and Joannopoulos[12] clearly elucidated, all the physical properties: We will, therefore, concentrate on the numerical advantages, which localized orbitals offer in dealing with the atomic relaxations leading to the annihilation of the dislocation pair.

In a conventional calculation, one has to calculate all the extended eigenorbitals to obtain the force acting on any single atom. This is clearly unnecessary if one wants to know only the forces acting on a subset of atoms. In this example, only atoms close to the dislocation pair will be displaced; for the atoms further away, the forces are not needed. In the localized-orbital method, the force acting on a certain atom depends only on the set of localized orbitals centered on itself [Eq. (10)]. It is, therefore, enough to calculate the localized orbitals belonging to those dynamic atoms, which will be significantly displaced. In addition, the relaxations can be done in a physically intuitive sequence of inward outward sweeps. In the first step of each sweep, one relaxes the atoms being close to the dislocation pair; in the second step, one relaxes the atoms somewhat further away and so on. In this way one obtains the final relaxed configuration much faster, since the force acting on the atoms, which are not nearest neighbors, is much larger in any step. The role of the static atoms far away from the vacancy, which are not displaced, is just to provide the correct scattering to the tails of the localized orbitals centered on the dynamic atoms and to indicate thereby, that the whole process takes place in a crystalline environment. Within a very simple-minded steepest-descent approach, we could in this way reduce the number of localized-orbital calculations required for the observation of the annihilation of the two dislocations from 300 000 to 200 000 for a 648-atom system.

TABLE I. Energies for a screw antiscrew pair at different separations as predicted by *ab initio* results (Ref. 12) for a 324-atom cell at the k point $\frac{1}{4}$, 0, 0, and by a 648- and 1296-atom TB calculation at the gamma point. All the energies are not corrected for stress and Madelung contributions.

	3.3 Å	9.9 Å	16.5 Å	23.1 Å
ab initio	4.36	7.70	10.76	13.32
TB 648	3.77	6.72	8.73	10.63
TB 1296	3.88	6.93	9.00	10.91

C. Molecular-dynamics simulations

As was already pointed out, this algorithm conserves the total energy in a MD simulation since the force given by Eq. (10) is the exact derivative of the approximate energy. This opens the possibility of microcanonical simulations. The microcanonical ensemble is not only the only thermodynamic ensemble that is well defined for finite systems, but it is also the easiest to implement. The force expression Eq. (10) assumes a constant chemical potential and the smooth electronic weight distribution corresponds to a finite electronic temperature. In this context, we do not attribute any physical meaning to a finite electronic temperature. In order to derive meaningful statistical quantities from a finite electronic temperature, the electronic density of states would need to represent the real properties of the system under consideration. This is, however, not the case with the present TB parametrizations. In addition, the broadening parameter $\Delta\epsilon$ of

the error-function weight distribution can be chosen rather high (in the eV range), which would correspond to unphysically high temperatures of some 10 000 K. The unique purpose of a finite electronic temperature is to stabilize the simulations. The same trick is also frequently used in density-functional calculations.[16] Instead of a finite electronic temperature, we will in the following, therefore, rather speak of a broadening.

Ordinary TBMD simulations are usually done for a fixed number of electrons and without broadening, even though it would be possible to do them also at constant chemical potential with broadening. In the fixed number case without broadening, the forces are given by

$$\mathbf{f}_\beta = \mathrm{Tr}\left[F_{\mu,T=0}(H)\frac{\partial H}{\partial \mathbf{R}_\beta}\right] = \sum_{i=\mathrm{occ}} \langle \Psi_i | \frac{\partial H}{\partial \mathbf{R}_\beta} | \Psi_i \rangle \ ,$$

where the chemical potential is adjusted in such a way as to give charge neutrality.

In the case of an insulator, the two settings (constant chemical potential with broadening, constant electron number without broadening) give almost identical results. As long as the chemical potential is in the gap and the broadening is sufficiently small, the number of electrons is constant since no levels can cross the gap and the valence-band levels are nearly fully occupied while the conduction levels are nearly empty. In the case of a metallic system, the two settings give rise to noteworthy differences. In the following, we will point out two quantities that are different in the two settings; namely, the electronic density of states near the chemical potential and the amplitude of fluctuations. In the following discussion, we will use the term chemical potential not only in connection with the true Fermi distribution, but also in connection with our complementary error-function electronic weight distribution, which was used for all calculations presented.

The conditions of constant electron number without broadening lead to a distortion of the density of states near the chemical potential and favor a large splitting between the highest occupied molecular orbital (HOMO) and lowest unoccupied molecular orbital (LUMO) states. The density of states for the two settings is shown in Fig. 9. For the constant electron number with no broadening setting, one sees a huge peak just below the chemical potential, which cannot be seen in the other setting and which seems unphysical. The HOMO-LUMO splitting is shown in Fig. 10. From the smoothed electronic density of states (see Figs. 7 and 9), one would expect for a disordered 64-atom system a HOMO-LUMO splitting of roughly 0.13 eV. This is actually roughly the splitting observed under constant chemical potential and broadening conditions. Under constant-electron-number no-broadening conditions, one finds however a splitting, which is roughly three times bigger than the expected one. These conditions, therefore, tend to make out of a metallic system a small-gap Jahn-Teller insulator: It is, therefore, to be expected that the metallic aspect is better described by the first setting. It is also noted that only in the constant chemical potential with broadening scheme can one observe crossings or avoided crossings of levels at the chemical potential. One might speculate that a simulation that prohibits eigenvalue crossings cannot explore the whole phase space.

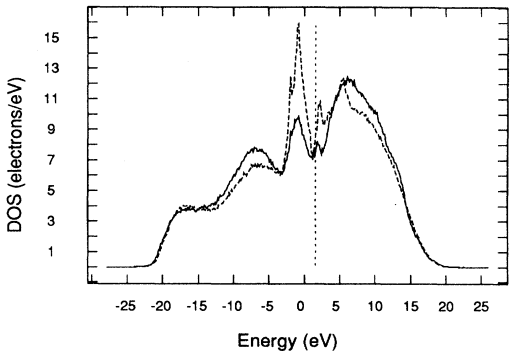

FIG. 9. The electronic density of states of a 64-atom carbon system averaged over 10 000 time steps for a simulation at the constant-potential with broadening (solid line) and the constant-electron-number setting without broadening (dashed line). The average chemical potential is indicated by dotted vertical line.

In the thermodynamic limit of very large metallic systems and for sufficiently low small broadening, the two settings approach the same limiting behavior. In the first setting, the fluctuations of the chemical potential become negligible; whereas in the second setting, the fluctuations of the electron number tends to zero and the conditions of constant chemical potential and constant electron number thus become identical. For small systems, the two settings are, however, different: Therefore, it does not make sense to compare forces or statistical quantities obtained with the two settings for small systems. The essential question is which setting approaches the limiting thermodynamic behavior faster. Unfortunately, it is not possible to answer this question by real calculations, since the numerical effort for the classical diagonalization

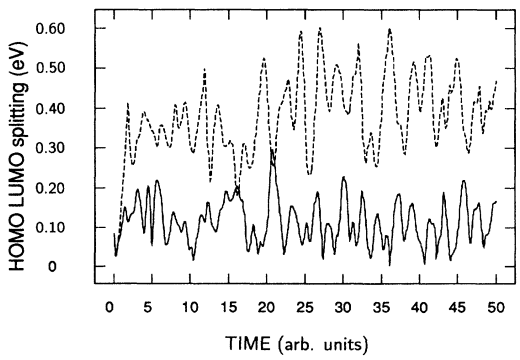

FIG. 10. The HOMO-LUMO splitting during a MD simulation for liquid C. The solid line shows the result at fixed chemical potential and finite electronic temperature; the dashed line shows the result for a fixed number of electrons without broadening. The starting configuration for the run was obtained under the first set of conditions.

would be prohibitive. It seems, however, reasonable to assume that the setting that dampens out fluctuations faster will more rapidly approach the thermodynamic limit. Let us now compare the fluctuations of the chemical potential and the fluctuations of the number of electrons in the two settings. Since we cannot directly compare these two quantities, we will translate the fluctuation of one quantity into a corresponding fluctuation of the other quantity. We choose to translate the fluctuation of the number of electrons in a fixed-chemical-potential simulation into a chemical-potential fluctuation. This is easily done by adjusting the chemical potential in molecular-dynamics simulation, where the forces are calculated under the assumption of constant chemical potential and with broadening at each step in such a way as to obtain overall charge neutrality. The result is shown in Fig. 11. It is clearly seen that the broadening leads to a considerable dampening of the fluctuations of the chemical potential.

These two observations suggest, therefore, that a constant-chemical-potential setting with broadening is better suited for molecular-dynamics simulations of metallic liquids because it gives a better electronic density of states and reduces the statistical fluctuations.

Let us finally still give some indications how to choose reliable parameters for a liquid-carbon simulation. The first important finding is that the value of $\Delta\epsilon$ can be as high in the metallic liquid as for solid diamond, namely 2 eV. Even though the system is metallic, its localized orbitals decay exponentially and this decay is independent of the value of $\Delta\epsilon$ as long as it is smaller than 2 eV. The exponential localization is, thus, not an artifact of the smooth Fermi distributions as it was the case for Al. This numerically helpful behavior can probably best be explained by the fact that even though the overall electronic density of liquid C looks metallic, the local density of states shows gaplike features. A value of $\Delta\epsilon$ larger than 2 eV leads, however, to an even stronger but now artificial exponential localization. Another important requirement is, according to our experience, that the fluctuations of the number of electrons on the Fermi surface, i.e., in the energy interval $[\epsilon-\Delta\epsilon;\ \epsilon+\Delta\epsilon]$ are small compared to the number itself. The ratio of the number of electrons on the Fermi surface to the number in the Fermi sea enters in the force expression and becomes visible in the quantities such as the correlation function. In Fig. 12, we show the pair-correlation function as obtained with three sets of parameters for a 1000-atom system. For this large system, the number of electrons on the Fermi surface is roughly 400. We see that changing $\Delta\epsilon$ from 2 to 1 eV has no visible effect as well as reducing the localization radius from 7.5 to 5.5 Å. Reducing the localization radius from 7.5 to 5.5 Å gives, however, a significant increase in the computational speed. The results are in good agreement with short-range data from other TB simulations[14] and Car-Parrinello[6,15] simulations.

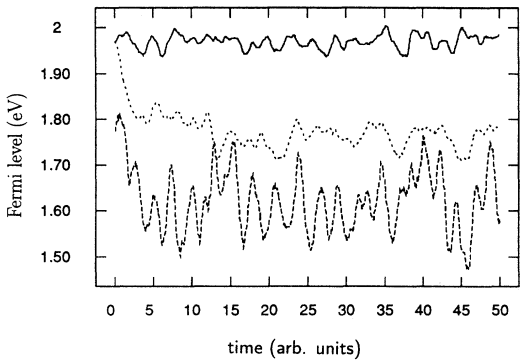

FIG. 11. The variations of the chemical potential during a MD simulation for liquid C. The solid curve shows the result if the forces are calculated at constant chemical potential with broadening but the chemical potential is nevertheless adjusted between the time steps such as to obtain charge neutrality. The dotted line shows the chemical potential calculated with broadening during a run where the forces are calculated at constant number without broadening. The full and dotted line would be nearly identical if the density of states were the same in the two settings. The dashed line shows the zero-temperature chemical potential (HOMO-LUMO midpoint) for a constant-number simulation without broadening.

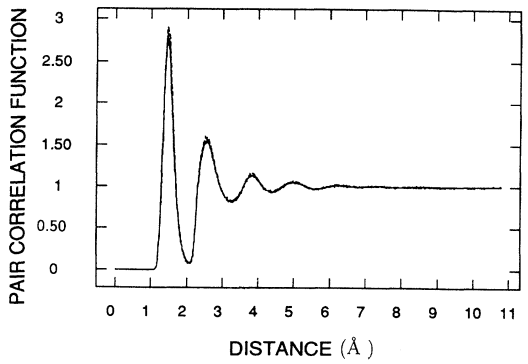

FIG. 12. The pair-correlation function for a 1000-atom sample of low-density liquid C at 5000 K as obtained with different parameters. First set: $\Delta\epsilon=1$, $r_{\rm loc}=7.5$ Å; second set: $\Delta\epsilon=2$, $r_{\rm loc}=7.5$ Å; third set: $\Delta\epsilon=1$, $r_{\rm loc}=5.5$ Å. The three curves are nearly indistinguishable.

VII. CONCLUSIONS

We described and analyzed in detail our algorithm for TB electronic-structure calculations and MD simulations. The algorithm is not only very efficient for both large insulating and metallic systems, but gives also a physically very intuitive approach to quantities such as energies and forces. In the case of metals, the smooth Fermi distribution leads to an artificial but numerically useful exponential localization of the localized orbitals. Even though the numerical workload is still considerable for large metallic systems such as defects and dislocations in metals, this algorithm allows us to study those systems. We have also demonstrated that it is preferable to use fixed-chemical-potential conditions with level broadening for MD simulations of metallic systems. For fixed-chemical-potential simulations, we obtain perfect energy conservation under any circumstances.

ACKNOWLEDGMENTS

We acknowledge computational support by the Cornell Theory Center (Ithaca, U.S.). One of us (S.G.) acknowledges financial support from Swiss and U.S. National Science Foundations. We thank T. Arias for providing us with his files containing the positions of the atoms around a screw dislocation and the different energy contributions, as well as interesting discussions on the problems of dislocations. We also thank both T. Arias and A. Horsfield for useful comments on our paper.

[1] *Many-Atom Interactions in Solids,* edited by R. M. Nieminen, M. J. Puska, and M. J. Manninen (Springer, Berlin, 1989); J. A. Majewski and P. Vogl, *The Structure of Binary Compounds* (North-Holland, Amsterdam, 1989), p. 287; T. A. Albright, J. K. Burdett, and M. H. Whangbo, *Optical Interactions in Chemistry* (Wiley, New York, 1985).

[2] L. Goodwin, L. Skinner, and A. J. Pettifor, Europhys. Lett. **9**, 701 (1989); L. Goodwin, J. Phys. Condens. Matter **3**, 3869 (1991).

[3] M. P. Teter, M. C. Payne, and D. C. Allan, Phys. Rev. B **40**, 255 (1989); T. A. Arias, M. C. Payne, and J. D. Joannopoulos, Phys. Rev. Lett. **71**, 1077 (1992).

[4] R. Car and M. Parrinello, Phys. Rev. Lett. **55**, 2471 (1985).

[5] G. Galli and M. Parrinello, Phys. Rev. Lett. **69**, 3547 (1992); F. Mauri, G. Galli, and R. Car, Phys. Rev. B **47**, 9973 (1993); P. Ordejon, D. Drabold, M. Grunbach, and R. Martin, *ibid.* **48**, 14 646 (1993); W. Kohn, Chem. Phys. Lett. **208**, 167 (1993); X.-P. Li, W. Nunes, and D. Vanderbilt, Phys. Rev. B **47**, 10 891 (1993); M. S. Daw, *ibid.* **47**, 10 895 (1993); W. Yang, Phys. Rev. Lett. **66**, 1438 (1991); M. Aoki, *ibid.* **71**, 1438 (1993); L-W. Wang and A. Zunger, Comput. Mater. Sci. **2**, 326 (1994).

[6] S. Goedecker and L. Colombo, Phys. Rev. Lett. **73**, 122 (1994).

[7] W. A. Harrison, *Electronic Structure and the Properties of Solids* (Dover, New York, 1989).

[8] W. Kohn, Phys. Rev. **115**, 809 (1959); J. des Cloizeaux, *ibid.* **135**, A698 (1964).

[9] D. Vanderbilt (private communication).

[10] R. Haylock and V. Heine, in *Solid State Physics: Advances in Research and Applications,* edited by D. Turnbull (Academic, New York, 1980), Vol. 35.

[11] S. Goedecker and L. Colombo, *Proceedings of the Supercomputing Conference, Washington, D.C., 1994* (SIAM, Philadelphia, 1994).

[12] T. A. Arias and J. D. Joannopoulos, Phys. Rev. Lett. **73**, 680 (1994).

[13] D. A. Drabold and O. F. Sankey, Phys. Rev. Lett. **70**, 3631 (1993).

[14] C. Z. Wang, K. M. Ho, and C. T. Chan, Phys. Rev. B **47**, 14 835 (1993).

[15] G. Galli, R. M. Martin, R. Car, and M. Parinello, Phys. Rev. Lett. **63**, 988 (1989).

[16] M. Weinert and J. W. Davenport, Phys. Rev. B **45**, 13 709 (1992).